This article has been accepted for inclusion in a future issue of this journal. Content is final as presented, with the exception of pagination.

Improvement of Short-Circuit Current Density in GaInP Solar Cells Grown by Dynamic Hydride Vapor Phase Epitaxy

Kevin L. Schulte, John Simon, Matthew R. Young, and Aaron J. Ptak

***Abstract*—We demonstrate GaInP solar cells grown by dynamic hydride vapor phase epitaxy with improved efficiency through elimination of nonradiative recombination centers. We redesigned our reactor to eliminate unintentional impurities, which led to a reduction of nearly 30× in dark current. This improvement led to a significantly improved open-circuit voltage of 1.41 V and a band gap-voltage offset of 0.47 V in a device with a rear reflector, achieved without front surface passivation. We demonstrate that the limiting factor toward achieving higher efficiency is control over the emitter thickness. Recombination is high in the unpassivated emitter, but losses can be minimized by designing it to be thin. We show that Se diffusion from the GaAs contact layer into the base is responsible for unintentional thickening of the emitter. Use of reduced contact doping reduces the penetration of Se into the p-GaInP base layer. With improved control of Se diffusion, we achieve 13.0 mA/cm^2 and 15.2% certified efficiency in a single-junction GaInP cell structure that is optically equivalent to the top cell in a GaInP/GaAs tandem.**

***Index Terms*—Photovoltaic Cells, III-V semiconductor materials, semiconductor growth, solar power generation.**

I. Introduction

III–V semiconductors exhibit the highest conversion efficiencies for single and multijunction solar cells [1], but are used in a limited set of applications because of high manufacturing costs [2]. Dynamic hydride vapor phase epitaxy (D-HVPE) is a potential route to reduced epitaxy costs for high-efficiency III–V devices, and D-HVPE-grown GaAs single junction cells are rapidly approaching the conversion efficiencies achieved by other growth techniques [3]. Tandem devices are necessary to fully leverage the benefits of III–Vs and push efficiencies significantly past those of silicon technology, which is approaching practical limits of just over 26% [4]. The record GaInP/GaAs tandem cell exhibits an efficiency of 32.8% [1] in a device grown by metalorganic vapor phase epitaxy (MOVPE), the principal III–V growth technology used in industry. We demonstrated a D-HVPE-grown GaInP/GaAs tandem solar cell with 23.7% efficiency without the benefit of a window layer [5], but increased current from the top cell is necessary to reach 30% or greater efficiency [5].

Previously, we demonstrated single-junction GaInP solar cells with 12.7% efficiency by D-HVPE [6], but the devices exhibited dark current behavior with $n = 2$ diode ideality. An $n = 2$ ideality implies that the bulk material quality, which is likely limited by deep level defects, limited device performance. Unintentional impurities [3] were responsible for the reduced performance in these devices. By carefully redesigning our custom D-HVPE reactor, we eliminated the source of impurities from the growth zone, which enabled us to deposit material with higher radiative efficiency. An unpassivated front surface, due to the absence of an Al source in our reactor that prevents development of high band gap passivation layers, presently limits the current of our devices. Modeling indicates that >14 mA/cm^2 is possible in an unpassivated structure with a 30-nm-thin emitter [5]. This current is enough to reach 30% in a GaInP/GaAs tandem while maintaining a reasonable one-sun sheet resistance [5].

In this paper, we detail recent advances in our GaInP solar cell devices designed for high-efficiency GaInP/GaAs tandems. We demonstrate GaInP cells with significantly reduced nonradiative defect density that are no longer limited by bulk material quality. We identify that control over the emitter thickness, which varies because of Se diffusion out of the GaAs contact layer, is the new limit on higher current collection in these devices. By reducing the Se doping in the GaAs contact, we improve our control over the emitter thickness, and demonstrate a device with an estimated emitter thickness of 70 nm. The device exhibits a short circuit current of 13.0 mA/cm^2 and a 15.2% (certified) efficiency under AM1.5G light illumination in a structure equivalent to a top cell in a GaInP/GaAs tandem (i.e., it receives no second pass of light from the rear reflector).

II. Experimental

Materials were grown in our dual-chamber, atmospheric pressure D-HVPE reactor, which utilizes rapid mechanical transfer to create doping or heterojunction interfaces [7]. GaInP solar cells were grown in an inverted fashion, initially with the structure and doping levels shown in Fig. 1. We employed a growth temperature of 650 °C, a V/III ratio of 4, and a ∼0.4 μm/min growth rate, unless noted. More complete growth details can

Manuscript received May 22, 2018; revised August 3, 2018; accepted September 12, 2018. This work is supported by the U.S. Department of Energy's Advanced Research Projects Agency – Energy (ARPA-E) under Award 15/CJ000/07/05. *(Corresponding author: Kevin L. Schulte.)*

The authors are with the National Renewable Energy Laboratory, Golden, CO 80401 USA (e-mail: kevin.schulte@nrel.gov; john.simon@nrel.gov; matthew.young@nrel.gov; aaron.ptak@nrel.gov).

Color versions of one or more of the figures in this paper are available online at http://ieeexplore.ieee.org.

Digital Object Identifier 10.1109/JPHOTOV.2018.2870938

2156-3381 © 2018 IEEE. Personal use is permitted, but republication/redistribution requires IEEE permission.
See http://www.ieee.org/publications_standards/publications/rights/index.html for more information.

Pursuant to the DOE Public Access Plan, this document represents the authors' peer-reviewed, accepted manuscript. The published version of the article is available from the relevant publisher.

This article has been accepted for inclusion in a future issue of this journal. Content is final as presented, with the exception of pagination.

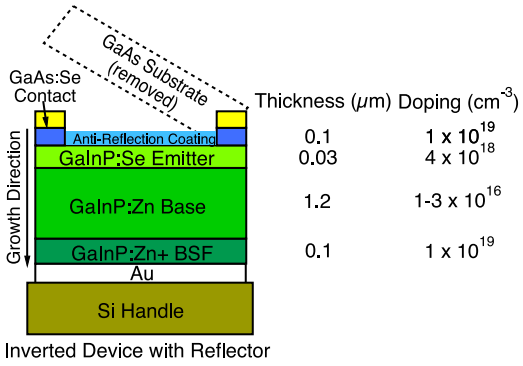

Fig. 1. Initial inverted GaInP solar cell structure targeted in this study. The gold back contact reflects unabsorbed light back to the base layer.

be found in [5] and [6]. The emitter was nominally designed to be 30 nm, although, as demonstrated below, this was not the case. The front surface is unpassivated, and a highly p-doped GaInP layer serves as the back surface field (BSF) and back contact layer. Later, devices were grown with a similar structure to Fig. 1, but with an absorbing GaAs contact layer or GaAs junction inserted between the BSF and the rear gold contact. The GaAs layer absorbs light that would otherwise reflect back into the base off of the gold, which simulates the optical environment experienced by a GaInP top cell in a GaInP/GaAs tandem device. All devices were 0.25 cm^2 in area. A MgF_2/ZnS antireflective coating (ARC) was applied to the surface of select devices. External quantum efficiency (EQE) and reflectance were collected using a monochromatic light source and broadband reference diode and used to calculate internal quantum efficiency (IQE). Current density–voltage (J–V) curves were measured under a calibrated AM1.5G spectrum, as well as in the dark. Secondary ion mass spectrometry (SIMS) was conducted on select samples to measure Se concentration, [Se], throughout the device structure. [Se] was quantified using Se implant standards in GaAs and GaInP to generate a relative sensitivity factor for Se in each material. The relative sensitivity factors were applied to the raw Se signal from the sample to calculate [Se]. Electroluminescence external radiative efficiency was measured as a function of injected current density and used to calculate an implied junction voltage [8], which enabled construction of dark J–V curves free of series resistance effects at higher currents.

III. Results and Discussion

Fig. 2 shows the EQE and reflectance (a) and the J–V characteristic under the AM1.5G spectrum (b) for two D-HVPE-grown GaInP cells with the structure shown in Fig. 1. HB318 is our previous best result [3], grown before the reactor reconfiguration. Compared with HC017, which was grown after the reconfiguration, it has slightly higher collection at longer wavelengths, in part due to a more optimal ARC, and a slightly lower band gap of 1.86 versus 1.88 eV. Thus, this cell has a short circuit current (J_{SC}) that is 1.2 mA/cm^2 higher. However, there is a marked difference in V_{OC}. HC017 has a V_{OC} of 1.41 V, an increase of 140 mV over HB318. The base doping of HC017 is slightly higher, 2.5×10^{16} versus 1.0×10^{16} cm^3, but not nearly enough

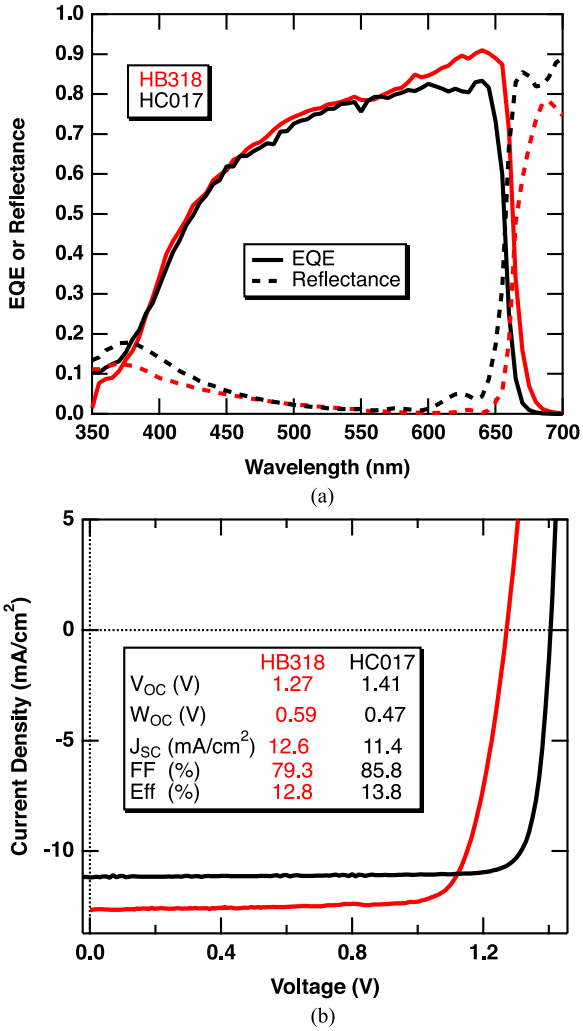

Fig. 2. EQE and reflectance (a) and light J–V characteristic under AM1.5G (b) for two GaInP devices grown before and after reconfiguration of the D-HVPE reactor.

to cause such a large increase in V_{OC}. This device has a band gap–voltage offset (W_{OC}) of only 0.47 V, despite a lack of front surface passivation. Fig. 3 shows the dark J–V characteristic for these two samples. Over a wide voltage range, the dark current for HC017 is $\sim$30$\times$ lower than HB318. In between these two growths, we substituted the stainless-steel cap that mates to the quartz reactor tube with a quartz cap, which resulted in a quartz/quartz seal and removed a potential source of iron from the reactor environment. We attribute the reduction in dark current to a reduction in unintentional deep level impurities related to this change. The large reduction in dark current leads to the significantly improved V_{OC} observed in HC017.

The ideality factor of the dark current (the slope on a semilog plot, as indicated by the broken lines in Fig. 3) provides information about the bulk material quality. An ideality of $n = 2$, which is not desirable, implies that bulk material quality is limiting the device behavior through Shockley–Read–Hall recombination at deep level traps in the depletion region [8], [9]. An ideality of $n = 1$ implies that recombination in the quasineutral regions of the device [9], which is typically related to radiative

Pursuant to the DOE Public Access Plan, this document represents the authors' peer-reviewed, accepted manuscript. The published version of the article is available from the relevant publisher.

This article has been accepted for inclusion in a future issue of this journal. Content is final as presented, with the exception of pagination.

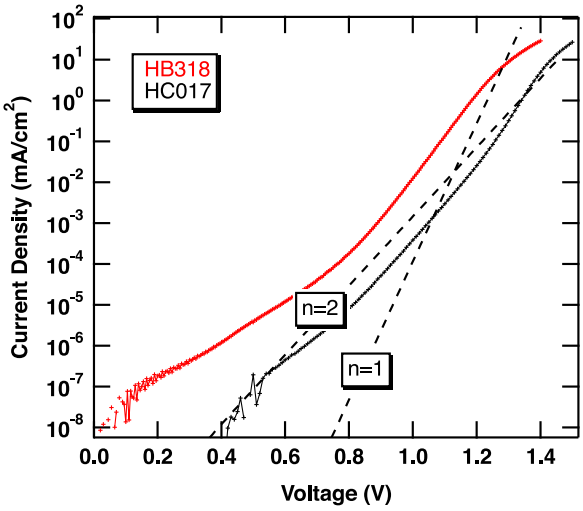

Fig. 3. *J–V* characteristic for the two GaInP devices in the dark.

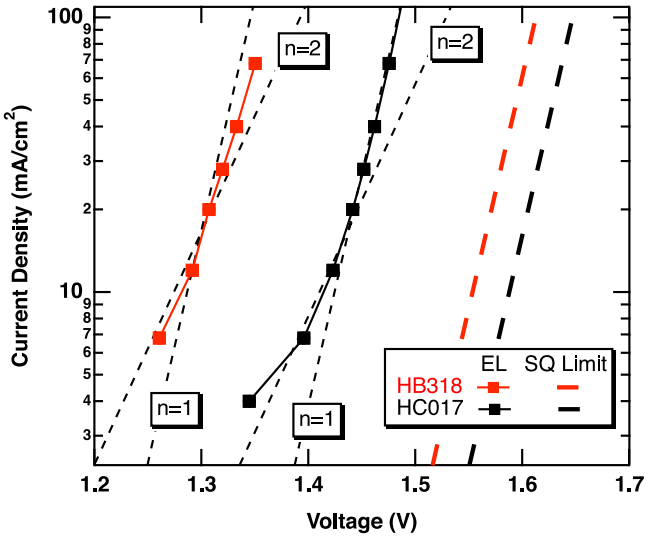

Fig. 4. *J–V* calculated from electroluminescence external radiative efficiency measurements. The thick broken lines indicate the expected behavior for a cell with perfect material quality and the band gaps of the specific devices. The thin broken lines indicate $n = 1$ or $n = 2$ diode behavior and are provided as a guide to the eye.

recombination mechanisms, dominates the *J–V* response. The ideality factor near V_{OC} in the dark *J–V* curves in Fig. 3 is not clear because of the effect of series resistance, which causes the curves to bend over at higher currents. We therefore plot the current density versus voltage calculated from the electroluminescence external radiative efficiency [8] in Fig. 4. By varying the injected current density and measuring the radiative emission, we can calculate an implied V_{OC} [8] and create a *J–V* curve. The ideality of these curves is more clearly discerned because this measurement is less sensitive to series resistance. Broken curves, which indicate the dark *J–V* behavior of an ideal material in the Shockley–Queisser (SQ) limit [8], [10] are also provided in the figure. HC017 transitions from an ideality of $n = 2$ to $n = 1$ very close to the one-sun current density of that device, while HC318 transitions much later and does not fully reach an $n = 1$ slope in the measured range. The concentration of

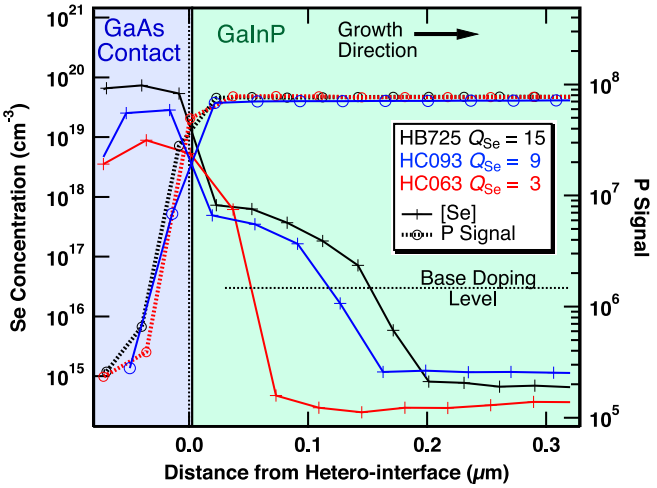

Fig. 5. SIMS [Se] for D-HVPE GaInP cell structures grown with varying Se dopant flow rates (Q_{Se}), in sccm, during growth of the GaAs contact layer. Se concentration is plotted on the left axis, while the P signal is plotted on the right to delineate the transition from GaAs to GaInP.

nonradiative defects in HC017 decreased to where it no longer controls the *J–V* response under one-sun operation.

Despite clear and significant reductions in defect density, the collection efficiency of HC017 as shown by EQE has not increased relative to HB318. The intended 30-nm emitter should be thin enough to sustain a QE of ~90% at 550 nm, even without front surface passivation [5], therefore something else must be limiting the QE. In this unpassivated device design, the QE is quite sensitive to the thickness of the emitter, since most carriers absorbed there recombine at surface states. Therefore, an unintentionally thick emitter would decrease the QE. We performed SIMS to look at the [Se] profile at the GaAs front contact/GaInP emitter interface as a function of 500 ppm H_2Se flow rate (Q_{Se}) during growth of the GaAs contact layer. Fig. 5 shows [Se] versus distance from this heterointerface for three values of Q_{Se} during contact growth, with all other growth parameters held constant. When $Q_{Se} = 15$ sccm, the value used in the two devices analyzed above, [Se] in the contact is nearly 10^{20} cm^{-3} and significant Se diffuses through the GaInP emitter and into the base. Se compensates the p-doped material, converting it to n-type material when [Se] increases above the p-type doping level in the base. [Se] is greater than the p-doping level in the base (~3×10^{16} cm^3) until ~150 nm past the GaAs/GaInP interface, which unintentionally thickens the emitter by ~5×· $Q_{Se} = 9$ leads to slightly less penetration of Se into the base, but the emitter still thickens to ~115 nm. A more abrupt doping profile is obtained for $Q_{Se} = 3$. For this flow rate, [Se] crosses the 3×10^{16} cm^3 threshold ~55 nm from the heterointerface, which yields an emitter thickness approaching the designed target of 30 nm. The doping concentration in the contact layer drops below 1×10^{19} cm^{-3} for this Q_{Se}, however, at which point the contact resistance may decrease the fill factor of the device. This tradeoff will be discussed below.

We then grew a series of GaInP cells, in which Q_{Se} during growth of the GaAs contact was the only parameter varied, to demonstrate the effect of Se diffusion on device QE. The

Pursuant to the DOE Public Access Plan, this document represents the authors' peer-reviewed, accepted manuscript. The published version of the article is available from the relevant publisher.

This article has been accepted for inclusion in a future issue of this journal. Content is final as presented, with the exception of pagination.

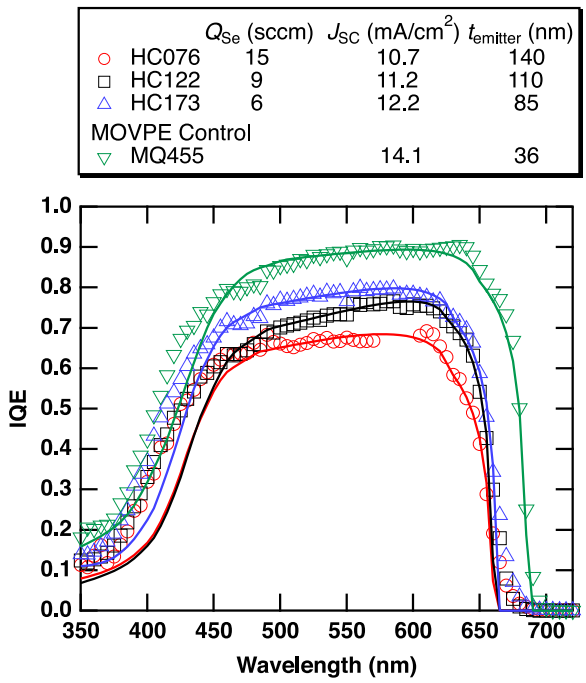

Fig. 6. (Markers) IQE as a function of Q_{Se} in the GaAs contact for GaInP cells grown as part of GaInP/GaAs tandems. IQE for a MOVPE-grown control cell with a 30-nm emitter, no front surface passivation, and a rear-absorbing GaAs layer is also provided. The J_{SC}s calculated by integrating IQEs with the AM1.5G spectrum are given in the table. Integration of the MOVPE IQE was cutoff at 1.87 eV, the band gap of the D-HVPE-grown cells. (Lines) Hovel-modeling of the experimental IQEs. The emitter thickness for which data were fit to the model is listed in the table.

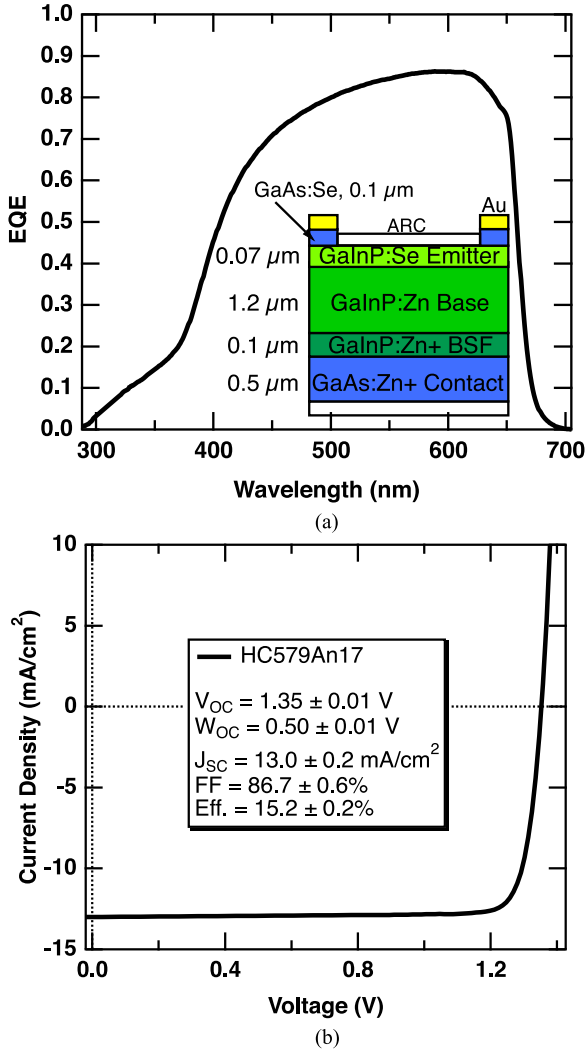

Fig. 7. (a) EQE for an optimized GaInP cell with absorbing GaAs layer between the cell and the rear gold contact. The cell structure is depicted in the inset. (b) *J–V* curve for this cell under AM1.5G illumination. The data in both panels were certified by the National Renewable Energy Laboratory Photovoltaic Device Performance Group.

device design is similar to that in Fig. 1, except that the cells were grown as part of inverted GaInP/GaAs tandems (see [5]). In this configuration, the GaAs subcell absorbs any light reflected from the rear gold contact and the contact layers are subjected to greater annealing than those analyzed in Fig. 2. A single-junction MOVPE cell was also grown with the same nominal structure and doping as in Fig. 1, but with a 0.5-μm-thick GaAs contact layer inserted between the BSF and the gold contact to absorb reflection from the gold. This cell provides a benchmark for the performance of the thin emitter top cell design we propose for a GaInP/GaAs tandem. Note that the MOVPE cell has a reduced band gap of 1.80 eV because of the presence of strong atomic ordering [11], which is not present to the same degree in the D-HVPE-grown samples. Fig. 6 shows the IQE of the D-HVPE series and the MOVPE cell. The IQE of the D-HVPE cells improves steadily with decreasing Q_{Se}, which confirms that Se diffusion through the emitter and into the base limits the QE, even at wavelengths near the band edge. We modeled the IQEs using Hovel's drift-diffusion model [5], [12], in order to estimate the effective emitter thicknesses of these cells (see Fig. 6, solid lines). We assumed similar device parameters as in [5], most notably a surface recombination velocity of 3×10^6 cm/s at the unpassivated emitter surface. The emitter thicknesses were adjusted to provide a best fit to the data. The estimated emitter thickness decreases from 140 to 85 nm in the range of contact doping tested. We note that the best fit for the MOVPE cell is a thickness of 36 nm, which is close to the nominal thickness of 30 nm. This cell employs a GaInAsN:Se front contact layer, which strongly binds Se and limits its diffusion [13]. Thus, this cell provides an excellent benchmark of what is achievable in an unpassivated GaInP cell when Se diffusion is repressed. Integration of the MOVPE cell IQE with the AM1.5G spectrum (cutoff at 1.87 eV, the band gap of the HVPE cells) yields a current of 14.1 mA/cm^2. If we can continue to thin the emitters of our D-HVPE cells and achieve this level of current, tandem efficiencies of 30% or greater are possible in an unpassivated cell design [5]. This is notable because it shows that high efficiency is possible in an Al-free design.

Finally, we demonstrate a single-junction D-HVPE-grown GaInP cell with a more optimal contact doping level of $Q_{Se} =$ 6 sccm, down from 15 sccm used for the cells in Fig. 2. This value is comparable to those used in the two-junction devices in Fig. 6, but note that the contact layer in this single-junction device is subjected to slightly less annealing load. The growth rate of this cell was ~0.9 μm/min and a V/III ratio of 4 was

Pursuant to the DOE Public Access Plan, this document represents the authors' peer-reviewed, accepted manuscript. The published version of the article is available from the relevant publisher.

This article has been accepted for inclusion in a future issue of this journal. Content is final as presented, with the exception of pagination.

employed. Fig. 7 presents the structure, EQE, and *J*–*V* of this cell. This cell also contains a GaAs contact layer behind the BSF to eliminate a second pass of light from the gold back contact, which mimicks the optical environment the cell experiences in a tandem configuration. The device exhibits a peak EQE of 86.3%, and QE modeling, like that employed in Fig. 6, indicates that the emitter thickness is 70 nm. The V_{OC} is 1.35 V, lower than the V_{OC} of HC017 in Fig. 2 for two reasons. First, the band gap is only 1.85 eV, which is roughly 20 meV lower than HC017, because of slightly higher In content. Second, the presence of the absorbing GaAs contact eliminates benefits related to concentration of an extra pass of light in the same cell volume as well as any photon recycling [8], [14]. Thus, the W_{OC} of this cell is 0.50 V. Despite the decrease in V_{OC}, we obtain an efficiency of 15.2% (certified by the National Renewable Energy Laboratory Photovoltaic Device Performance Group) under AM1.5G illumination because the J_{SC} increased to 13.0 mA/cm^2.

This result is promising because it implies that $>$14.0 mA/cm^2 is within reach if we can continue to thin the emitter. The obvious route to a thinner emitter is to continue reducing the contact doping. We note that the contact resistance of this cell, obtained by transfer length measurement, is only 0.135 mΩ/cm^2 and the fill factor is nearly 87%, which implies that the contact doping is still high enough to provide a low loss contact for a one-sun device. Another solution would be necessary in the event that further reductions in the contact doping start to negatively affect the fill factor, however. Based on the diffusion behavior demonstrated in Fig. 5, the diffusion front is much more abrupt at contact doping levels of 1×10^{19} cm^{-3} or below. A thicker contact with intentionally graded doping, such that the concentration is 1×10^{19} cm^{-3} or above at the metal/semiconductor interface but lower than that closer to the GaInP device layers, presents a promising option. The eventual performance of this unpassivated device design is not fundamentally limited by the contact resistance, however.

IV. Conclusion

We demonstrated GaInP solar cells grown by D-HVPE with significantly improved material quality through the reduction of nonradiative defects. We presented a device with a W_{OC} of only 0.47 V despite an unpassivated front surface and demonstrated that nonradiative defect density is no longer the main limiting factor to device efficiency. Rather, we found that unintentional thickening of the emitter caused by Se diffusion out of the GaAs contact into the GaInP base layer limited the QE and J_{SC}. The thicker emitter significantly reduced collection because of the surface recombination rate in that unpassivated layer. We showed that it is possible to achieve $>$14.0 mA/cm^2, a threshold that enables a 30% GaInP/GaAs tandem, in an unpassivated, thin emitter device grown by MOVPE. Using improved understanding and control of Se diffusion, we demonstrated a $J_{SC} = 13.0$ mA/cm^2 and 15.2% efficiency in a D-HVPE-grown GaInP device without a rear reflector.

Acknowledgment

The authors would like to thank David Guiling and Waldo Olavarria for materials growth, and Michelle Young and Daniel Lu for device processing. This work was authored by the National Renewable Energy Laboratory, operated by Alliance for Sustainable Energy, LLC, for the U.S. Department of Energy (DOE) under Contract No. DE-AC36-08GO28308. The information, data, or work presented herein was funded by the Advanced Research Projects Agency (ARPA-E), US Department of Energy. The views expressed in the article do not necessarily represent the views of the DOE or the U.S. Government. The U.S. Government retains and the publisher, by accepting the article for publication, acknowledges that the U.S. Government retains a nonexclusive, paid-up, irrevocable, worldwide license to publish or reproduce the published form of this work, or allow others to do so, for U.S. Government purposes.

References

[1] M. A. Green *et al.*, "Solar cell efficiency tables (version 51)," *Prog. Photovolt. Res. Appl.*, vol. 26, no. 1, pp. 3–12, 2018.
[2] K. A. Horowitz, M. Woodhouse, H. Lee, and G. P. Smestad, "A bottom-up cost analysis of a high concentration PV module," in *AIP Conf. Proc.*, vol. 1679, no. 1, 2015, Art. no. 100001.
[3] J. Simon *et al.*, "Upright and inverted single-junction GaAs solar cells grown by hydride vapor phase epitaxy," *IEEE J. Photovolt.*, vol. 7, no. 1, pp. 157–161, Jan. 2017.
[4] D. D. Smith *et al.*, "Toward the practical limits of silicon solar cells," *IEEE J. Photovolt.*, vol. 4, no. 6, pp. 1465–1469, Nov. 2014.
[5] K. L. Schulte, J. Simon, and A. J. Ptak, "Multijunction $Ga_{0.5}In_{0.5}P$/GaAs solar cells grown by dynamic hydride vapor phase epitaxy," *Prog. Photovolt. Res. Appl.*, pp. 1–7, 2018, doi: 10.1002/pip.3027.
[6] K. L. Schulte *et al.*, "Development of GaInP solar cells grown by hydride vapor phase epitaxy," *IEEE J. Photovolt.*, vol. 7, no. 4, pp. 1153–1158, 2017.
[7] K. L. Schulte *et al.*, "Computational fluid dynamics-aided analysis of a hydride vapor phase epitaxy reactor," *J. Crystal Growth*, vol. 434, pp. 138–147, 2016.
[8] J. F. Geisz, M. A. Steiner, I. Garcia, S. R. Kurtz, and D. J. Friedman, "Enhanced external radiative efficiency for 20.8% efficient single-junction GaInP solar cells," *Appl. Phys. Lett.*, vol. 103, no. 4, 2013, Art. no. 041118.
[9] C.-T. Sah, R. N. Noyce, and W. Shockley, "Carrier generation and recombination in P-Njunctions and P-Njunction characteristics," *Proc. IRE*, vol. 45, no. 9, pp. 1228–1243, 1957.
[10] W. Shockley and H. J. Queisser, "Detailed balance limit of efficiency of P-N junction solar cells," *J. Appl. Phys.*, vol. 32, no. 3, pp. 510–519, 1961.
[11] T. Suzuki, A. Gomyo, and S. Iijima, "Strong ordering in GaInP alloy semiconductors; Formation mechanism for the ordered phase," *J. Crystal Growth*, vol. 93, no. 1, pp. 396–405, 1988.
[12] H. J. Hovel, "Solar cells," in *Semiconductors and Semimetals*, R. K. Willardson and A. C. Beer, Eds. New York, NY, USA: Academic Press, 1975, vol. 11, pp. 8–47.
[13] M. A. Steiner, J. F. Geisz, R. C. Reedy, and S. Kurtz, "A direct comparison of inverted and non-inverted growths of GaInP solar cells," in *Proc. 33rd IEEE Photovolt. Spec. Conf.*, 2008, pp. 1–6.
[14] M. Steiner *et al.*, "Optical enhancement of the open-circuit voltage in high quality GaAs solar cells," *J. Appl. Phys.*, vol. 113, no. 12, 2013, Art. no. 123109.

Authors' photographs and biographies not available at the time of publication.

Pursuant to the DOE Public Access Plan, this document represents the authors' peer-reviewed, accepted manuscript. The published version of the article is available from the relevant publisher.